Biomaterials Science: Processing, Properties and Applications III.
Edited by Susmita Bose, Amit Bandyopadhyay and Roger Narayan.

PROCESSING AND BIOACTIVITY EVALUATION OF ULTRAFINE-GRAINED TITANIUM

A. Thirugnanam[a], T.S. Sampath Kumar* and Uday Chakkingal

Department of Metallurgical and Materials Engineering, Indian Institute of Technology Madras, Chennai, Tamil Nadu, INDIA 600036.
[a] Presently at Department of Biotechnology and Medical Engineering, National Institute of Technology Rourkela, Odisha, INDIA 769008.

ABSTRACT

Titanium has been the material of choice for hard tissue replacements due to its excellent biocompatibility and high strength to weight ratio. Since, cells live in a nano-featured environment of extracellular matrix; there is great interest in the formation of submicron to nano size grain materials over conventional biomaterials. Equal channel angular pressing, groove pressing and mechanical milling of commercially pure titanium (cpTi) was carried out to obtain submicron/nano grain size materials. The processed samples were characterized using optical microscope, scanning electron microscope (SEM), X-ray diffraction (XRD), transmission electron microscope (TEM), hardness, tensile properties, atomic force microscope (AFM), and contact angle measurements. Microstructural and mechanical characterization of the processed samples exhibited grain refinement and improved mechanical properties when compared to as received condition. The bioactivity study of the fine grained samples in SBF exhibited dense and homogenous apatite layer on the surface. All samples were found to be non-toxic by MTT [3-(4, 5-Dimethylthiazole-2-yl)-2, 5-diphenyl tetrazolium bromide] assay to fibroblast cells and culture study using osteoblast cells show more cell adhesion and spreading on ultra fine grained samples compared to as received cpTi. The enhanced bioactivity in the fine grained samples is due to submicron/nano surface features with high wettability and surface energy.

INTRODUCTION

Pure titanium and titanium alloys are now the most attractive metallic materials for biomedical applications [1]. Ti–6Al–4V has been a main biomedical titanium alloy for a long period and is the most widely used material for medical implants. However, Al and V in the alloy are considered to be potentially toxic. Hence commercially pure titanium (cpTi) is more attractive in biomedical applications for load bearing site if its strength is increased to that of Ti6Al4V [2]. The morphology of the biomaterial is critical to its success as implants, because cells attach, organize, and grow well around fibers with diameters smaller than those of the cells in their natural environment, i.e. cells live in a nano-featured environment of a complex mixture of pores, ridges, and fibers of extracellular matrix (ECM). This information eventually leads to the concept of nanobiomaterials and perceived to be beneficial over conventional biomaterials.

Severe plastic deformation (SPD) processes has become very attractive over the last decade because of its potential for achieving considerable grain refinement, typically to the submicrometer or nanometer level [3, 4]. Equal channel angular pressing (ECAP), accumulative roll bonding, high pressure torsion, groove pressing (GP) and mechanical milling are some of the common SPD techniques used to obtain submicron/nano grain size materials [5-8]. Equal channel angular pressing (ECAP) has been increasingly recognized due to the unique physical

and mechanical properties inherent in various ultra fine grained materials. The deformation mode in ECAP under ideal condition is 'simple shear' and the plastic deformation in the ECAP work piece is very homogeneous and the dimension of the sample does not change after the process. Groove pressing (GP), was developed for fabrication of plate-shaped ultra fined grained metallic materials without changing their initial dimensions [9]. Groove pressing is carried out such that a gap between the upper die and the lower die is same with the sample thickness, the inclined region of the sample is subjected to pure shear deformation under plane strain deformation condition. A die design with the groove angle (θ) of 45° yields a shear strain of 1 at deformed region for a single pressing. Ball milling is used to synthesize nanocrystalline materials. The advantage of using ball milling for the synthesis of nanocrystalline materials lies in its ability to produce bulk quantities of material in the solid state using simple equipment and at room temperature [8]. Hence, it has been planned to obtain ultra fine grain structures on cpTi by ECAP, GP and mechanical milling and to evaluate its *in-vitro* bioactivity for a possible enhancement. ECAP was conducted at warm and at room temperature conditions. Ball milling was carried out with pure titanium powder as well as with various combination of titanium and hydroxyapatite mixture.

MATERIALS AND METHODS

Commercial pure titanium supplied by MIDHANI, India was used as the starting material. The chemical composition of the material is Fe 0.01%, Cl 0.076%, N 0.004%, O 0,027%, Si 0.002%, Ni 0.009%, C 0.004% and balance titanium. The as recieved, ECAP warm worked, ECAP room temperature, groove pressed, ball milling of pure titanium and ball milling of titanium and HA composite were coded as AR, EW, ER, GP, BMT and BTH respectively.

ECAP at warm working (EW) was carried out at 400 °C up to 3 passes (coded as EW1P, EW2P, EW3P for 1st pass, 2nd pass and 3rd pass respectively) following route B_c (i.e., rotating the sample 90 degree clockwise after consecutive pass). The die used was 17 mm diameter with 120° die angle. ECAP at room temperature (ER) was done only up to 2 passes (coded as ER1P, ER2P for 1st pass and 2nd pass respectively) in 120° die angle following route B_c.

Commercial pure titanium sheets of 2mm thickness were GP using molybdenum-di-sulphide as the lubricant. The deformed sheet was removed from the dies and flattened between a set of flat dies. After flattening, the sample was rotated by 180 degree about an axis perpendicular to the plane of the sheet and second pressing was done using the grooved dies which constitutes one pass. The groove pressing at room temperature was continued up to 3 passes (coded as GP1P, GP2P and GP3P for 1st pass, 2nd pass and 3rd pass respectively) beyond which the specimen exhibited cracks on the surface.

Commercially pure titanium powder with 300 mesh size was ball milled in a tungsten carbide closed vial with 10mm diameter balls. Ethanol was used as the wetting medium. The powder to ball mass ratio was 1:20 and the rotation speed was maintained at 200 rpm. Milling was done for various time intervals (4, 8, 12, 16, 20 and 24 h). Different compositions of nano HA (10, 15 and 20 wt. %) and micron sized HA (20 wt. %) were ball milled with pure titanium and were coded as BTH90n10, BTH85n15, BTH80n20 and BTH80m20 respectively. Milling was done for different time intervals (4, 8, 12 and 16 h) for each condition. The as milled powder was characterized by XRD, SEM and TEM. The milled samples were compacted and sintered in a vacuum sealed quartz tube at 900°C for 2h. Porosity studies were done on the sintered compacts using mercury intrusion porosimeter (MIP, AutoPore IV1.08, Micromeritics, USA).

The sintered compacts were then immersed in simulated body fluid (SBF) for up to 4 weeks to access its bioactivity.

The hardness (432SVA Wolpert Vickers hardness) and tensile properties (INSTRON 8800, UK) of AR and processed (ECAP and GP) samples were measured. The optical microstructures of AR cpTi and processed samples (ECAP and GP) were observed using optical (LECCIA) microscope and image analysis software for measuring the grain size. The average grain size of AR cpTi was found to be 50 microns.

Scanning electron microscope (SEM, FEI Quanta 200, Holland) observations were performed to study the morphology of ball milled powders. The morphology of apatite for all the processed samples when immersed in SBF for 2 and 4 weeks were also observed using SEM. From the bioactivity studies, the Ca/P ratio of the apatite formed was quantified using elemental analysis. SEM was also done to observe the morphology and spreading of osteoblast cells adhered for 2 and 4 days of culture. The cell cultured samples were gold sputter coated (about 5 nm thick) and then observed in SEM. Transmission electron microscopy (TEM, Philips CM12, Holland) was done on the processed samples (ECAP and GP) to study the submicron features. In case of ball milled samples, the powder was double dispersed in methanol using an ultrasonicator and then observed in TEM using a carbon coated copper grid. Selected area diffraction (SAD) patterns were obtained using large aperture. The surface morphology of ECAP and GP samples were observed using an atomic force microscope (AFM, Dimension 3100, Nanoscope IV digital instruments, USA) in contact mode. Section analysis of the AFM image was also obtained.

Contact angle measurements (GBX Digidrop contact angle meter, France) were carried out on ECAP and GP samples with distilled water as the contacting solvent. Six measurements were done for each condition. The measurements were made after allowing the droplet on the sample surface for 30 seconds. From the contact angle measurements, the surface energy was calculated using the following equation [10]:

$$E_s = E_{vl} \cos\theta \qquad \text{----------} \quad (1)$$

where, E_{vl} is the surface energy between water and air under ambient condition, (i.e., 72.8 mJ/m^2 at 20 °C) for pure water and θ is the static contact angle. The pore size of BM sintered samples was measured using the MIP.

The ultra fine grain refined samples (ECAP, GP and BM) were evaluated for bioactivity by immersing them in SBF for up to 4 weeks [11]. After immersing in SBF the samples were washed in distilled water and observed in SEM. The apatite formed is also confirmed using XRD. Cytotoxicity test was done to determine the cell viability using L929 (mouse fibroblast subcutaneous connective tissue) cell line procured from National Centre for Cell Sciences, Pune, India. The cells were maintained in RPMI 1640 (Himedia, Pune, India) medium supplemented with 10% foetal bovine serum (Sigma, USA) and 100 IU/ml penicillin and 100 lg/ml streptomycin (medical grade). The culture was incubated at 37°C in a humidified atmosphere containing 5% carbon dioxide for 24 hours in a culture plate of 24 wells. The absorbance of the colored solution can be quantified by measuring at a certain wavelength (usually between 500 and 600 nm) by a plate reader (spectrophotometer). For osteoblast cell adhesion studies samples in triplicate were conditioned with sufficient volume of media in a 24 wells culture plate. Human osteoblast cells were adhered on the surface of processed samples. The cells (5000 cells/cm^2)

were seeded on the surface of the samples and then media was added along the sides of the wall so that cell suspension will be on the top of the material. The culture plate was then incubated for 30-45 min in CO_2 incubator. Then sufficient amount of media was added and then incubated for 2 and 4 days. The cover slip was observed under light microscope after 2 and 4 days. The samples were then removed and processed for SEM analysis.

RESULTS AND DISCUSSION

The hardness values of ECAP and GP titanium is shown in Figure1. The values reported were the average of ten measurements. It was observed that ER samples showed higher hardness values than EW samples. The increase in hardness at room temperature may be due to strain hardening at cold working conditions. The hardness of GP1P sample increased to 190 HV as a result of strain hardening. After second pass, the hardness of GP sample increased slightly (203 HV) and then decreased to 182 HV at third pass. The decrease in hardness in subsequent GP may be due to dislocation annihilation as a result of strain path reversal between successive passes. It is now well established that the hardness of ultra-fine grained materials is significantly higher than coarse grain material. The tensile properties of AR, ECAP and GP samples are given in Table I. The results showed that the tensile ductility of AR sample was initially high but dropped due to severe plastic deformation. The yield strength increased drastically for EW process and then gradually increases with number of passes. The tensile properties of ER samples were not determined as the extruded specimens were not long enough to machine a tensile specimen as per ASTM E8. The ECAP samples showed highest strength as compared to other conditions. The tensile properties of GP samples also improved which is due to strain hardening and grain refinement.

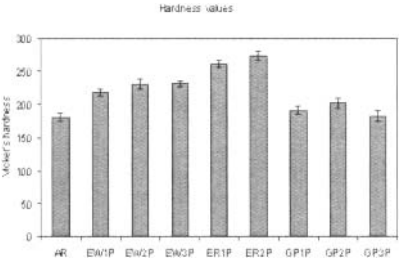

Figure 1. Vickers hardness of bulk processed sample

The optical micrograph of AR, EW3P, ER2P and GP3P samples were shown in Figure 2. The initial grain size of the AR sample was approximately found to be 50μm. From the micrographs, it is evident that there is considerable grain refinement than AR condition. The GP3P sample shows the presence of large volume of twins within grain. When compared to ECAP process, GP did not exhibit effective grain refinement as the strain imposed in the sample was much high in ECAP process. Figure 3 shows the TEM micrograph of EW3P and ER1P sample. The micrographs in Figure 3a is composed of elongated bands having widths of ~300 nm for EW3P and 1.6 μm for ER1P samples; and within these bands there are high densities of dislocations formed into irregular cell structures. The SAED pattern of ER1P (Figure 3b) shows the formation of ring indicating high angle grain boundaries.

Table I. Tensile properties of bulk processed samples

Processing conditions	0.2 YS (MPa)	UTS (MPa)	% Elongation
AR	320	450	30
EW1P	680	700	21
EW2P	720	780	18
EW3P	745	814	15
GP1P	400	523	25
GP2P	432	537	21
GP3P	445	548	20

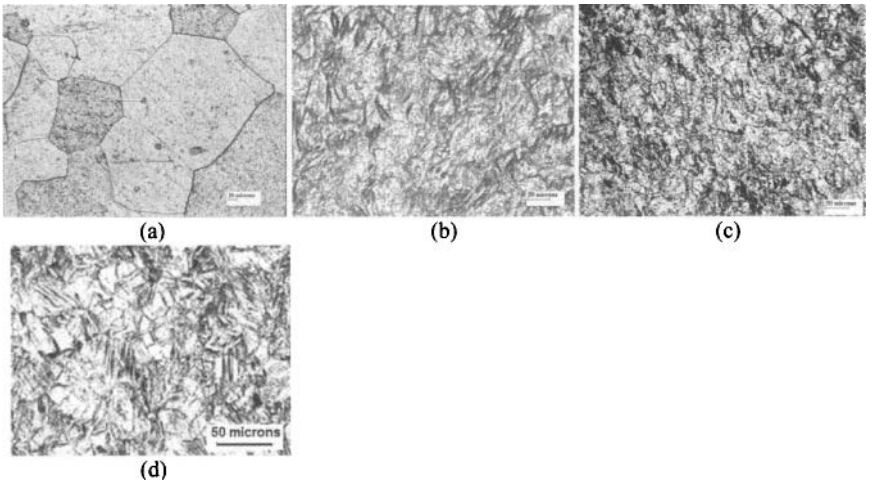

Figure 2. Optical micrographs of (a) AR sample (b) EW3P sample (c) ER2P sample (d) GP3P sample.

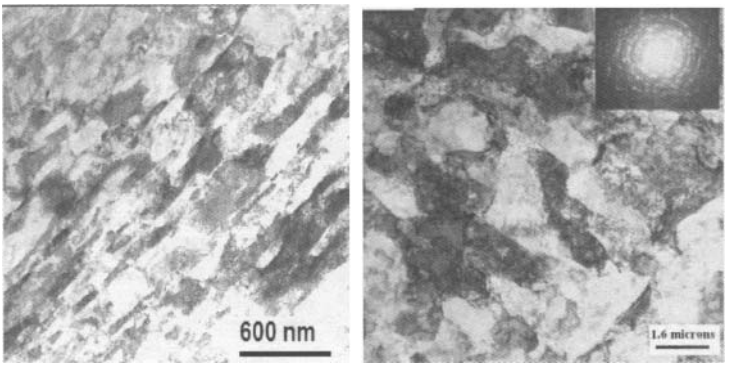

Figure 3. TEM micrographs of (a) EW3P and (b) ER1P samples

The atomic force microscope (AFM) was done to measure the surface features of ECAP and GP samples. Figure 4 shows typical AFM image of AR, EW3P and GP3P samples. It was observed that the surface features of the processed samples contained submicron bumps. These surface features are similar to the refined grains that were observed in TEM. These surface features play an important role in enhancing apatite nucleation. When an implant material is placed inside a human body, among the plethora of events that take place the first and the foremost one is the wetting of the implant material by the physiological fluids. This further controls the adsorption of proteins followed by attachment of cells to the implant surface. Hence, surface wettability is considered as an important criterion that can dictate the biocompatibility of the implant material. The three most important factors that affect the wettability of a surface are its chemical composition, microstructural topography, and surface charge. Contact angle measurements are probably the most adopted technique to measure the average wettability of a surface. The processed samples (ECAP and GP) showed relatively hydrophilic surfaces compared to AR samples, i.e. less than 50 deg of water contact angles. The surfaces of ultra fine grain cpTi had significantly lower water contact angle (38 degree) than coarse-grain (49 degree) titanium and showed greater surface energy. The value reported were average of six measurements. The enhanced surface energy due to high wettabillty improves cell adhesion thus adhering more proteins and cells.

All the processed samples (ECAP and GP) were immersed in SBF to study its bioactivity for up to 4 weeks. Figure 4 also shows SEM micrographs of AR, EW3P and GP3P samples immersed in SBF for 4 weeks. It was observed that all the ultra fine grain refined samples had more apatite nucleated on its surface when compared to AR sample for the same time period immersed in SBF. The enhanced apatite nucleation is due to grain refinement which results in more grain boundary area than the coarse grained titanium. The morphology of the apatite was found to be dense and globular for all ultra fine grain samples. The dense apatite formed was around ~250 μm thick. The Ca/P ratio calculated from EDX was found to be 1.66 which is close to that of human mineral bone phase.

Ball milling of cpTi and cpTi-HA after various time interval were subjected to XRD analysis to check if there is any phase or contamination formed during milling. The XRD pattern of ball milled titanium at various time intervals for cpTi (TBM) and cpTi-HA (BTH90n10) is shown in Figure 5. It is found that the diffraction peaks became broader with increase in milling time, indicating the reduction in crystallite size. The powder particles tend to get cold welded to each other, especially if they are ductile, due to heavy plastic deformation experienced and then fractures during milling. During the initial stage of ball milling, cold welding is predominant than fracturing as the material is ductile. There should be a balance maintained between cold welding and fracturing of particles. Hence ethanol is added to the vials which act as surface active agents, adsorbs on the surface of the powder particles and minimizes cold welding between powder particles and there by inhibits agglomeration. It also acts as a coolant and avoids excessive heat formation during ball milling. Titanium oxide peaks were observed after 24h of ball milling of cpTi (TBM). At 24h the peaks were broadened and the oxide content increased with increase in milling time. This may be due nano sized crystallite having more surface area and entrapment of atmospheric air into the vial during sample loading. Nitrogen and oxygen are the two major compositions of atmospheric air which adsorbs on the newly created surfaces due to repeated fracture and cold welding during ball milling and diffuse into powder matrices through defects such as grain boundaries and dislocations. However, the formation enthalpies for

TiN and rultile TiO_2 are -346.89 $kJmol^{-1}$ and -959.75 $kJmol^{-1}$ respectively at standard conditions. Hence TiO_2 should be easily formed than TiN at standard conditions [12].

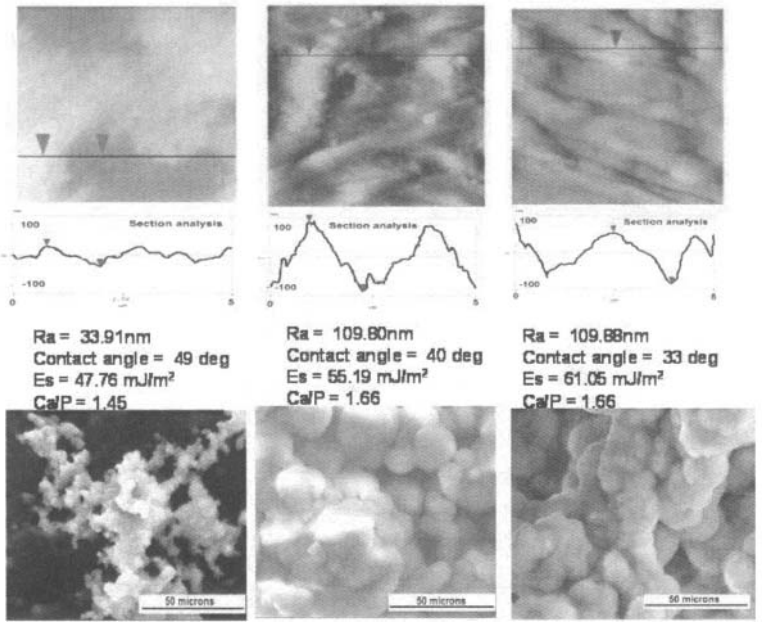

(a) **(b)** **(c)**

Figure 4. Comparison of AFM images, surface roughness, contact angle, surface energy, Ca/P ratio and SEM images showing in-vitro bioactivity when immersed in SBF for 4 weeks (a) AR (b) EW3P and (c) GP3P samples.

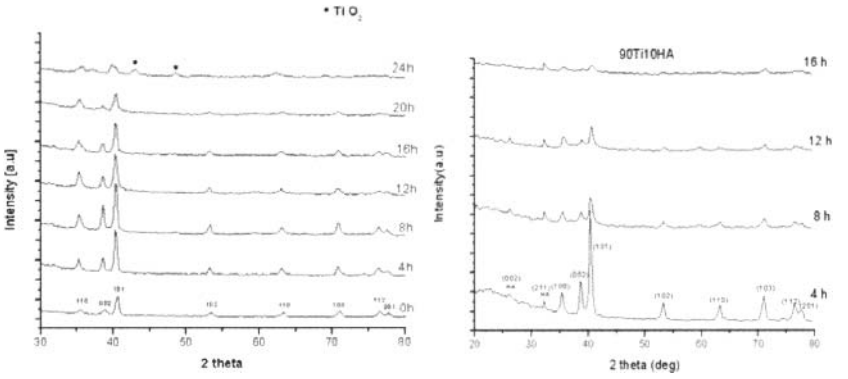

(a) (b)

Figure 5. XRD of ball milled samples at various time intervals (a) pure titanium (b) 90Ti10HA

The morphologies of the samples milled at different time intervals were observed by SEM. The particle size for the BMT sample milled at 20h and BTH80n20-16h is shown in Figure 6. The reduction in particle size during ball milling is due to repeated fracture and cold welding as a result of heavy plastic deformation. Work hardening takes place and the particles become less ductile and fracture easily at higher milling time. The EDX at various milled time interval showed that the oxide content increased with increase in milling time. The diffusion of oxygen into titanium matrix results in TiO_2, a brittle phase which can be fractured easily. However, TiO_2 is also bioactive and a small amount of it occurring during ball milling is unavoidable.

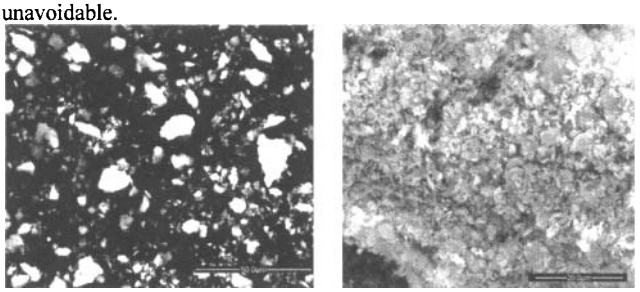

(a) (b)

Figure 6. SEM micrographs of ball milled (a) BMT-20h (b) BTH80n20-16h

The morphology of ball milled samples was also observed by TEM. Figure 7a shows the dark field image of BMT-20h and Figure 7b shows the bright field image of BTH80n20-16h ball milled samples. It was observed that the milled particles were agglomerated for BMT-20h and BTH80n20-16h. This may be due to high surface energy of ball milled powder which tends to agglomerate the nano crystallites. The dark field image of the milled particles shows white spots in the agglomerated titanium particles, which indicates the presence of nano sized particles. Selected area electron diffraction (SAED) pattern (Figure 7c) revealed that the diffraction spots were diffused to form a ring pattern which confirms the presence of nano crystallites.

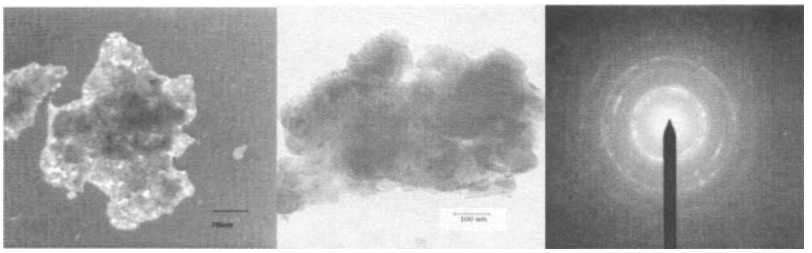

(a) (b) (c)

Figure 7. TEM micrograph of ball milled samples: (a) dark field image of BMT-20h (b) bright field image of BTH80n20-16h (c) Typical SAD pattern for condition b

The bioactivity of sintered compacts (BMT and BTH) was accessed by immersing it in SBF for up to 4 weeks. It was observed that the apatite formed on the surface of ball milled sintered pellets also showed dense and homogenous coatings similar to that of processed (ECAP

and GP) bulk cpTi samples. This apatite forming process can be interpreted in terms of the surface charge. The treated titanium metal is initially negatively charged, and hence combines with positively charged calcium ions in SBF to form a calcium titanate. As the calcium ions are accumulated, the surface is positively charged and hence combines with negatively charged phosphate ions to form an amorphous calcium phosphate with low Ca/P ratio (~1.48). This phase is metastable and hence eventually transforms into crystalline bone-like apatite with Ca/P ratio almost similar to that of bone (~1.66). From the EDX analysis the atomic weight % of Ca/P ratio was found to be 1.66 which is close to the composition of bone. A typical SEM micrograph for BMT-20h and BTH80n20-16h samples immersed in SBF for 4 weeks is shown in Figure 8. The apatite nucleations of BTH samples were much homogenous and denser than BMT samples for the same time period when immersed in SBF. From the MIP, the interstitial porosity of BMT milled for 20h and BTH80n20 samples milled for 16h was found to be 42% and the average pore diameter was found to be 30μm. The HA which is already present in BTH composite and the porous structure resulted in enhanced nucleation of apatite when immersed in SBF.

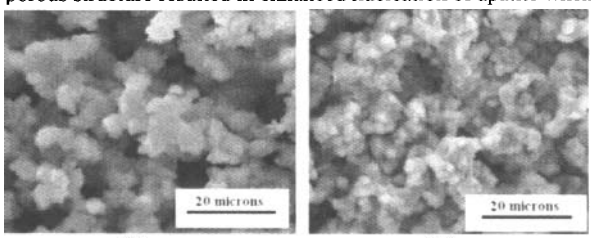

(a) (b)

Figure 8. SEM micrograph showing bioactivity when immersed in SBF for 4 weeks (a) BMT-20h (b) BTH80n20 -16h

For conducting the cell culture studies the sample which induced more apatite nucleation in SBF studies was selected from each processing condition. Four samples namely AR, GP3P, BMT-20h and BTH80n20-16h were chosen for cell culture studies. For cytotoxicity test, L929 cells were seeded on the selective grain refined samples for 24 hours and MTT assay is added to study the activity of enzymes. DMS (dimethyl sulfoxide, an acidified ethanol solution) was added to dissolve the insoluble purple formazan product into a colored solution. The culture plate is then inserted in a spectrophotometer. The readings obtained from the plate reader are shown in Table II. From the table, it is evident that all the 4 selective samples show more than 80 % of viability. Generally, viability above 60 % is considered to be non-toxic. Hence from the cytotoxicity study it is concluded that cpTi processed through various severe plastic deformation techniques were non-toxic and further cell adhesion studies using human osteoblast cells can be conducted.

For osteoblast cell adhesion, human osteoblast cells (5000 cells/cm^2 surface area) were seeded on the surface of the samples and then media was added along the sides of the wall so that cell suspension will be on the top of the material. The culture plate was then incubated for 30-45 min in CO_2 incubator for 2 and 4 days. The samples were then processed using various grade of alcohol for SEM analysis. It was observed that osteoblast cells adhered more on all ultra fine grain refined samples when compared to AR titanium for 2 and 4 days of incubation (Figure 9). The increase in adhesion is due to submicron/nano surface features on all the processed samples [13,14]. The number of osteoblast cells adhered and spread on day 4 was found to be more when compared to 2 days of incubation (Figure 10). It was observed that most of the cells

exhibited advanced stages of spreading i.e cells exhibiting cytoplasmic webbing and fully spread. [15]. Thus, increased wettability caused by high-energy grain boundaries and the presence of abundant submicron-grain structures favourable for osteoblast adhesion seemed to contribute to the early osteoblast cell response on. In case of porous samples, BTH80n20-16h ball milled sample showed advanced stages of cell spreading than BMT-20h after 4 days of incubation. From this it is evident that cpTi with submicron features forms better integration with bone in *in-vivo* condition.

Table II. Cytotoxicity studies shows percentage of cell viability using L929 cells

Conditions	Sample code	Spectrophotometer reading (Sample number, N)			% cell viability (Sample number, N)		
		1	2	3	1	2	3
AR	**A**	1.924	1.871	1.870	97.96	95.26	95.28
GP3P	**D**	1.834	1.839	1.822	93.38	93.63	92.76
BMT- 20h	**E**	1.877	1.733	1.805	95.57	88.24	91.90
BTH80n20-16h	**F**	1.658	1.581	1.707	84.00	80.04	86.91

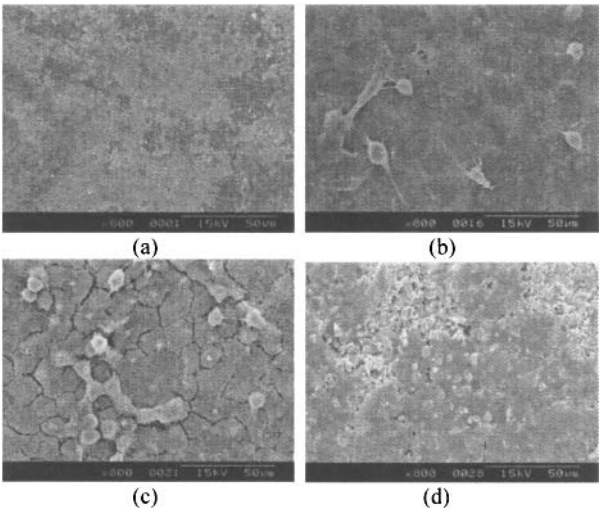

Figure 9. SEM images of osteoblast cells adhered for 2 days on (a) AR (b) GP3P (c) BMT-20h and (d) BTH80n20-16h.

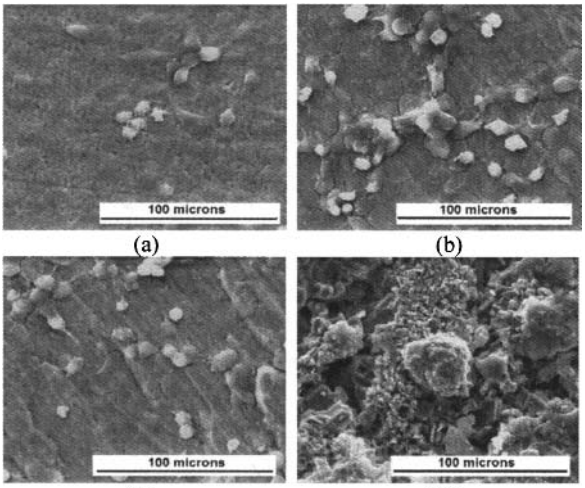

Figure 10. SEM images of osteoblast cells adhered for 4 days on (a) AR, (b) GP3P (c) BMT-20h and (d) BTH80n20-16h

CONCLUSIONS

From this study, equal channel angular pressing and groove pressing exhibited ultra fine grains with enhanced strength as well as bioactivity. However, a combination of equal channel angular pressing followed by cold rolling process increased strength to that of Ti6Al4V so that it can be used in load bearing sites. The bioactivity of this combined process also showed dense and homogenous apatite with Ca/P ratio close to that of HA stoichiometry. The enhanced strength and bioactivity is due to high surface wettability and surface energy. Porous titanium and Ti-HA composite synthesized by ball milling showed excellent bioactivity. However, Ti-HA composite exhibited much dense and homogenous apatite than pure titanium. From the MTT assay studies using L929 fibroblast cells, it was evident that all the processed samples were non toxic with more than 80% of cell viability. Human osteoblast cells showed better adhesion on submicron grain sized titanium when compared to coarse grained titanium for 4 days of incubation. The ultra fine grain refined samples (ECAP, GP and BM) showed advanced stages of spreading exhibiting cytoplasmic webbing.

REFERENCES

1. D. M. Brunette, P. Tengvall, M. Textor and P. Thomsen, *Titanium in Medicine*, Springer – Berlin, Heidelberg, NewYork, 2001.
2. M Niinomi, Mechanical properties of biomedical titanium alloys, *Materials Science and Engineering A*, **243,** 231-36 (1998).
3. R. Z. Valiev, R. K. Islamgaliev and I.V. Alexandrov, Bulk nanostructured materials from severe plastic deformation, *Progress in Materials Science*, **45 (2),** 103–89 (2000).
4. V. M. Segal, Materials processing by simple shear, *Materials Science and Engineering A,* **197 (2),** 157–64 (1995).

5. Y. H. Chung, J. W. Park and K.H. Lee, An Analysis of Accumulated Deformation in the Equal Channel Angular Rolling (ECAR) Process, *Metals and Materials International* **12 (4),** 289–93 (2006).
6. H. R. Song, Y. S. Kim and W.J. Nam, Mechanical properties of ultra fine grained 5052 Al alloy produced by Accumulative Roll-Bonding and Cryogenic Rolling, *Metals and Materials International,* **12 (1),** 7–13 (2006).
7. A. Thirugnanam, T.S. Sampath Kumar and Uday Chakkingal, Tailoring the bioactivity of commercially pure titanium by grain refinement using groove pressing, *Materials Science and Engineering C* **30(1),** 203-08 (2010).
8. C. Suryanarayana, E. Ivanov and V.V. Boldyrev, The science and technology of mechanical alloying, *Materials Science and Engineering A*, **304–306,** 151–58 (2001).
9. D. H. Shin, J. J. Park, Y. S. Kim and K.T. Park, Constrained groove pressing and its application to grain refinement of aluminium, *Materials Science and Engineering A*, **328,** 98–103 (2002).
10. D. Khang, J. Lu, C. Yao, K. M. Haberstroh and T. J. Webster, The role of nanometer and sub-micron surface features on vascular and bone cell adhesion on titanium. *Biomaterials*, **29(8),** 970-83 (2008).
11. T. Kokubo and H. Takadama, How useful is SBF in predicting in vivo bone bioactivity, *Biomaterials*, **27,** 2907-15 (2006).
12. C. J. Lu, J. Zhang and Z.Q. Li, Structural evolution of titanium powder during ball milling in different atmosphere, *Journal of Alloys and Compounds*, **381,** 278-83 (2004).
13. S. Faghihi, A. P. Zhilyaev, J. A. Szpunar, F. Azari and H. Vali, Nanostructuring of a Titanium Material by High-Pressure Torsion Improves Pre-Osteoblast Attachment, *Advanced Materials*, **19,** 1069-79 (2007).
14. T. J. Webster and J. U. Ejiofor, Increased osteoblast adhesion on nanophase metals:Ti, Ti6Al4V, and CoCrMo, *Biomaterials*, **25,** 4731–39 (2004).
15. R. Rajaraman, D. E Roundsa, S.P.S Yenb and A. Rembaumb, A scanning electron microscope study of cell adhesion and spreading in vitro, *Experimental Cell Research,* **2,** 327–39 (1974).